Phys. Status Solidi C 9, No. 6, 1378–1383 (2012) / DOI 10.1002/pssc.201100705

physica status solidi c
www.pss-c.com
current topics in solid state physics

Graphene and graphane functionalization with hydrogen: electronic and optical signatures

A. I. Shkrebtii[*,1,2], E. Heritage[1], P. McNelles[1], J. L. Cabellos[2,3], and B. S. Mendoza[2]

[1] University of Ontario, Institute of Technology, Oshawa, ON, L1H 7L7, Canada
[2] Centro de Investigaciones en Optica, Leon, Guanajuato 37150, Mexico
[3] Universidad del Pais Vasco, 20018 Donostia-San Sebastian, Spain

Received 9 October 2011, revised 13 December 2011, accepted 17 December 2011
Published online 14 March 2012

Keywords graphene, graphane, partial hydrogen passivation, band gap tuning, optical properties

* Corresponding author: e-mail Anatoli.Chkrebtii@uoit.ca, Phone: +1-905-721-3050, Fax: +1-905-721-3304

We proved the possibility of electron gap tuning of graphene-based materials, using extensive first principles modelling of the structural, electronic and optical properties of *partially* hydrogenated graphene. Optical tools were proposed to characterize the hydrogenation process. Sub-monolayer hydrogen passivated graphene and various hydrogen induced superstructures were considered. Electron and optical DFT LDA gaps between 0.2 and 1.8 eV, suitable for microelectronic application, were obtained for low hydrogen coverage structures. For such systems, hydrogen clustering (by saturating neighbouring C dangling bonds at opposite sides of the graphene sheet) is energetically most favourable and generally produces a larger gap. A more homogeneous H distribution with one-side bonding to C-host atoms is, in contrast, less energetically favourable and even structurally unstable. In addition, such H configurations generally produce lower electron band gap. Hydrogen at low coverage not only locally buckles six-fold carbon rings, it leads to dimerization and subsequent electron localization for neighbouring carbon atoms, which are not H bonded. Such structural and electronic processes are responsible for gap opening and its magnitude. Calculated linear optical response indicates that the optics is not only gap sensitive, but, combined with experimental spectra, can also provide access to microscopic properties of 2D nano-sheets such as symmetry, hydrogen induced structure, degree of hydrogenation, chemical bonding, and others.

1 Introduction Since 2004 we have witnessed a spectacular growth in research on graphene, a new class of 2D nanomaterial [1], which exists both in a stable free standing form as well as on a top of various semiconducting surfaces [1-4] or metallic substrates [5]. Despite the fact that graphene was known for decades as a convenient mathematical and physics model (see, for instance, [6]), a general consensus was that free standing atomic monolayer films should be intrinsically unstable and therefore could not be created in reality (for details see [7] and refs. therein). One of the main outcomes of a simple micromechanical cleavage experimental procedure proposed in [1], however, was that one can actually produce such a material and investigate its properties experimentally. Graphene is one atom thick 2D layer of carbon atoms arranged in a honeycomb lattice with sp^2 hybridized bonds: each C has three neighbours in the xy plane. The remaining p_z orbitals are delocalized along the plane, offering unusual and exciting electronic properties of this material. In particular, graphene is a semimetal with zero electron band gap and demonstrates record high electron conductivity due to a linear band dispersion of the delocalized p_z electrons in a vicinity of Fermi level (the so-called Dirac cone bands). However, graphene's semimetallic nature with zero-band gap excludes it from *p-n*-junction based applications in 2D microelectronics. The presence of the forbidden zone is required for creating *p-n* junctions in such devices as transistors, active region of solar cells, *etc*. More complex graphene based systems as quasi free-standing multilayers at SiC surfaces [2-3], SiO_2 [5,8] or metal surfaces, such as Ir(111) [4] have their electron structure modified by the interaction with the substrate or between the layers. Such interaction, however, cannot create sufficient for microelectronic devices energy gap. Therefore, since graphene dis-

covery, modification of the material's property by chemical functionalization, extra confinement, *etc*., has attracted a lot of attention (for a very recent review see [9]).

However, as it was first demonstrated theoretically in 2007 [10], complete hydrogenation of graphene is possible, which produces a stable free standing film, graphane, with the most stable energetically the so-called chair structure. Two years later such fully hydrogenated graphene has been synthesized experimentally [7]. By saturating all p_z bonds of graphene, hydrogen pulls carbon atoms out of the plane, thus producing sp^3 hybridization of carbon atoms, which results in the electron gap opening. Formation of sp^3 hybridization, which buckles the carbon host atoms, instead of flat sp^2 is the mechanism responsible and required for transformation of the semimetallic graphene into graphane. Graphane, however, can be classified as a wide band gap insulator rather than semiconductor because of its large (above 5 eV, [11]) band gap. This again makes impossible the creation of suitable for application in "carbon-based electronics" *p*-*n*-junctions based on graphane films.

Since the first papers on graphene demonstrated its unique properties, a lot of efforts were made to create graphene based non-zero gap semiconductor rather than insulator type of materials. For instance, one can exploit possibilities of the gap opening in graphene or, in contrast, reducing the graphane's gap. As an example, adding extra confinement to graphene within its plane creates the so called nano-ribbons [12,13]. The gap openings achieved, however, were below 0.1 eV, which is not sufficient for microelectronic applications. Confinement in two directions of the plane leads to graphene based quantum dots [14], but still with similar narrow band gap. Apart from ribbons creating by, *e.g.,* cutting of the graphene plane, ordered partial hydrogenation was proposed [15,16], that actually affects electrons by confinement of the narrow graphene strip with selectively hydrogen covered areas. However, to open the gap close to those of Si or GaAs, the confinement mechanism was not sufficient. As the result, a hot topic in both experimental and theoretical research is directed toward engineering graphene based systems with a tunable gap by using different impurities for the free standing films [9,17], a few graphene layers [18] or graphene on various substrates [19]. Many promising for microelectronics application systems can be obtained from graphene using the simplest adsorbate, hydrogen [20].

In order to tailor the gap of one atomic layer thin carbon films as well as silicon and germanium graphene's analogues, we have theoretically suggested controlled partial hydrogenation of graphene, graphene-like silicon (silicene) and germanium (germanene) systems [21]. Similar idea was also proposed theoretically for graphene in [15] using the partial hydrogenation of graphene. Independently, the effect of partial graphene hydrogenation was observed experimentally for free standing graphene films [22], and for the film deposited at the Ir(111) substrate [23]. This confirmed a possibility of graphene band structure modification by submonolayer H coverage.

It is important to be able to comprehensively and noninvasively characterise such systems *in-situ* during the preparation process and application. Raman spectroscopy is one of the tools of choice for characterisation of the H passivated graphene at different coverages [8]. This method and infrared (IR) spectroscopy, however, are not sensitive to the electron gap opening. To characterise the electron gap modification optical spectroscopies, such as ellipsometry of reflectances anisotropy spectroscopy (RAS) can be used. In addition, RA measurements can be crucial when the ordering of hydrogen (intentional [15] or driven by total energy minimum [16]) is present: both graphane and graphene are optically isotropic along the plane, thus producing no optical anisotropy. The same is valid if the partially deposited hydrogen in randomly distributed along the surface. However, ordering of impurities will lead to nonzero RA signal.

In [24] we further demonstrated a possibility of electron gap tuning of graphene-based materials by extensively modelling numerous (more than 20) partially hydrogenated graphene superstructures with 75%, 50%, 25%, 12.5% and 6.25% of monolayer (ML) coverage. We focused there on electron band structure, electronic density of states (DOS) and vibrational spectra for the above partially hydrogenated systems. In agreement with other theoretical finding [17,18], our structural optimization demonstrated that the graphene film is rippled (or buckled) when hydrogen saturated p_z bonds. We have found, however, that the local buckling or its average over the supercell, as an intuitive measure of the gap opening, do not demonstrate any trend, (Fig. 6(a) from [24]). Furthermore, we did not find a clear correlation between the electron gap opening and degree of hydrogenation (Fig. 6(b) from [24]). Therefore, to uniquely characterize the modification of the electron properties and especially the band gap in partially hydrogenated systems, other microscopic mechanisms should be considered.

In this paper we focus on detailed analysis of the microscopic physics of partial hydrogenation process and, especially, mechanisms of the gap opening for only a few most promising structures obtained in [24]. The discussion here is mostly based on the analysis of calculated electron charge density and linear optical properties, required to decode experimental optical response of the hydrogenated material. Optical techniques, and especially differential methods [25], allow very accurate, quick and non-invasive *in-situ* probes of numerous properties of various systems in both fundamental and applied research. To use optics as a characterization tool for the systems of interest, we calculate linear dielectric tensor along *x*, *y* and *z* directions and its anisotropy, which is the difference in light absorption for different light polarizations. This is intended to predict (RAS) spectra in terms of microscopic hydrogen arrangement. Although in the current research we also calculated and analyzed band structure and the Projected Density of States (PDOS), important for device application, the current analysis is based on discussion of the atomic structure, charge density and reflectance anisotropy.

2 Technical details Density Functional Theory (DFT) within the Local Density Approximation (LDA) plane-waves and pseudopotentials scheme as implemented in Quantum Espresso (QE) package [26] was used. The repeated slab geometry with periodic boundary conditions (PBC) and 22 Å thick vacuum layer (sufficient to decouple wave functions of the neighbouring carbon sheets) were used to realistically describe 2D systems. 40 Ry and 65 Ry cutoffs were used for structure determination and up to 65 Ry for calculating the optical properties. The Plane Wave (PW) mode of QE, which allows accurate multiple *k*-points Brillouin zone sampling, was used for atomic structure optimization, electron and optical properties. Ab-initio Born-Oppenheimer molecular dynamics (BOMD) also with a large set of *k*-points was used to extract the vibrational frequencies. The geometry optimization is achieved through relaxation of the structure toward its total energy minimum. Band structure, density of states (DOS), projected DOS (PDOS), joint DOS (JDOS) and linear optical response (the imaginary part of dielectric tensor) were calculated. Although band structures were considered for most of the supercells studied, we mostly used DOS and JDOS for our analysis because hydrogen should be randomly distributed in the partially hydrogenated samples, apart from a few special cases of adsorbate ordering. Hence, the band structure is not a well defined parameter for disordered systems.

The primitive graphene cell contains two atoms and our structures of interest were modelled using hexagonal and rectangular supercells with their size ranging from 2 to 16 primitive unit cells and thus containing up to 32 carbon host atoms with extra H atoms bonded to C.

It should be noted that DFT LDA underestimates the band gap compared to the experimental value. This is a well known problem and there are techniques to correct it, including accurate many-particle GW corrections (see, *e.g.*, [11]) or reasonably accurate but simple so-called "scissors operator", which rigidly shift the energy of the empty surface states up by a well defined amount. Important is that despite the underestimation of the energy gap, DFT LDA produces the correct electron wave functions for both filled and empty states. Hence, we consider here only DFT LDA results. We do not consider excitonic effects, their contribution (which is numerically expensive) can modify the optical curves [11], but adding these effects will not change the main physics mechanisms relevant to the processes that we are interested in.

Average buckling and dimerization of the host carbon atoms for partially hydrogenated graphene were calculated. We define here buckling as the average of the absolute value of the vertical shifts of each C atom from its original position in a flat graphene plane. The dimerization was calculated as the average absolute changes in C bond distances

We considered in [24] hydrogen–graphene interfaces in the range from 75% to 6.25% of H monolayer (ML) and numerous hydrogen induced superstructures. In contrast to [24], we discuss here in details only a few most typical and representative structures. In particular, we demonstrate here the main physical mechanisms of partial hydrogenation by using one of the most promising structure types, which we named "$C_{16}H_2$ row close". It has two hydrogen atoms bonded to two neighbouring carbon atoms, and located at opposite sides of the sheet and represents the most stable geometry with 12.5% of hydrogen. We start, however, with properties of two other systems with 50% hydrogenation, named #1 (H atoms are at two sides of C host) and #2 (H at one side only). We name the $C_{16}H_2$ system as #3. These three structures are shown in Fig. 1 together with graphane (#4).

3 Results: atomic structure *vs.* electron charge density We start with the physics of hydrogen passivation. When hydrogen is bonded to the carbon atoms of a graphene sheet, this pulls the C atoms out of the plane by producing sp^3 hybridization instead of sp^2 in graphene. When all carbon atoms are H-passivated (each C is connected to one H, which corresponds to 1 ML coverage), every p_z electron has become completely *localized* and graphane is formed with a buckling of 0.23 Å and an electron band gap above 5 eV [11]. During *partial* graphene hydrogenation, an H atom also locally buckles a plane with C atoms, bonded to this hydrogen. It is important to stress that such "buckling perturbation" usually (but not always) propagates through the carbon plane involving C atoms which are not H connected. Such perturbations are largest in the vicinity of the carbon atoms bonded to hydrogen. However, contrary to intuitive expectation, the buckling and corresponding formation of sp^3 bonding configuration does not always lead to the electron gap opening. Another crucial mechanism, involved in band structure modification, is the *dimerization* of the remaining C atoms, which are not H saturated. We illustrate these conclusions considering two different 50% H passivated and the 12.5% hydrogenated $C_{16}H_2$ system mentioned above.

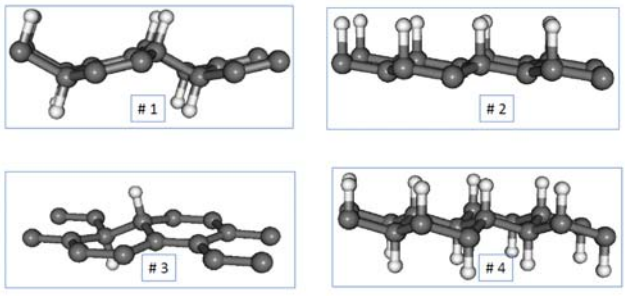

Figure 1 Perspective view of the H passivated graphene systems considered. Corresponding H coverage is 50% for structures #1 and #2. Structure #3 contains 12.5% of H, while graphane (#4) is 100% H passivated.

The structure #1 contains 25% of H monolayer above the C host plane and 25% below (see Fig. 1, upper left panel) and the second structure #2 (upper right panel) has

50% of hydrogen only at the top of the C plane. The lower panel at the left of Fig. 1 shows $C_{16}H_2$ structure #3 with 12.5% of hydrogen. Finally, at the bottom, right graphane chair structure (#4) is shown for comparison.

We list the main structural and electron properties of the three partially hydrogenated systems considered in Table 1 together with graphene and graphane for comparison. The table includes the optical gap E_G, average buckling and average dimerization of C atoms.

Completely hydrogenated graphene, that is graphane (structure # 4 in Fig. 1), has C–C bond length equal to 1.49 Å, C–H bond length of 1.12 Å, while C atoms plane buckling is 0.23 Å and DFT LDA band gap of 3.12 eV. Interatomic distance in graphene, namely C–C bond length is 1.42 Å, which is noticeably less than for graphane. Our DFT LDA band structure, and DOS (not shown here) are in perfect agreement with that of DFT LDA, calculated, *e.g.*, in [11].

Structure #1 is the most energetically stable among 50% hydrogenated systems studied [24]. In this structure, H is bonded to opposite and neighbouring C-host atoms and forming a row along [1-10] direction (we use three-axis system, similar to that one of ideally terminated C(111)1×1 surface [27], p. 151). C–H bonds are tilted with respect to normal z direction. The other half of C atoms, which are not H connected, create parallel rows as well. This produces hydrogen ordering, thus offering the possibility of transforming 2D graphene to an array of 1D nanowire. It is important to stress that DFT LDA electron gap for such a system is 3.58 eV, which is *higher* than that of 3.12 eV for graphane.

Table 1 Structural and electronic properties of the partially hydrogenated superstructures under consideration. Energy gap E_G, carbon atoms' average buckling and dimerization as well as the optical gap are compared to graphene and graphane.

H (%)	Structure	Energy gap E_G, eV	Average buckling, Å	Aver. dime- riza- tion, Å
0	Graphene	0.0	0.0	0.0
50.0, #1	$C_{16}H_8$	3.58	0.28	0.11
50.0, #2	$C_{16}H_8$ up	0.0	0.12	0.00
12.5, #3	$C_{16}H_2$	1.43	0.07	0.04
100, #4	Graphane	3.12	0.23	0.00

Hydrogen adsorption in structure #1 produces strong local buckling of half of the carbon atoms, which are directly bonded to H: vertical C atoms separation is 0.79 Å (larger that in graphane) and C–C bond length is 1.57 Å, 5% larger than in graphane. On the other hand, there is a flat-like arrangement of the rest of C atoms, which are not H connected. Here C-H bond length is very similar to that of graphane and equals to 1.12 Å, while the bond length between H-connected C and H-free C atoms is 1.48 Å, close to that of graphane. Finally, H-free C–C distances are drastically shortened compared to graphene or graphane: the C–C bonds are only 1.35 Å long, which is 10% contracted compared to graphane and 5% less than in graphene. Such large contraction of the H-free carbon atoms indicates a strong *dimerization* of carbon atom pairs. In addition to σ-bonds in the C-plane, such dimerization creates an extra bond due to a strong π interaction. This will be clearly demonstrated next by using the calculated charge density for the structures under consideration.

Structure # 2 with H only at the one side of the carbon sheet is strikingly higher in total energy by 0.512 eV per one atom compared to structure #1, while H atoms are bonding to every other C atom: hydrogen bonding to the neighbouring C is mostly unstable energetically. H bonding at one side of graphene produces reasonably large buckling, equal to 0.12 Å, while average distance between C atoms is 1.49 Å, close to that for graphane. Considering such a buckling and interatomic distances one can intuitively expect the band gap opening. However this system is a poor metal: there is a group of states inside the gap with the Fermi level localized in the center, which demonstrates metallic character. These states are the half filled localized p_z dangling bond states at the bottom of the structure and their appearance can explain higher total energy compared to the structure #1. Being not saturated, this leads to the overlap of the filled and empty states and their metallic character. However, electron motion is limited only by jumps between these half filled but distant π states, which makes the material only slightly conducting. This is markedly different from graphene conductivity mechanism.

Finally, $C_{16}H_2$ structure (#3) represents most stable low (12.5%) H covered and functionalised system. Hydrogen bonding to the two C neighbours at the opposite sides of the carbon sheet is most energetically favourable, producing local buckling of 0.34 Å, while the average buckling for this structure is only 0.07 Å (compared to zero buckling for graphene and 0.23 Å for graphane). Average dimerization of the atoms is 0.04 Å. The optical gap of such low H coverage system is only 1.43 eV, which demonstrates semiconducting character and indicate on a possibility of a band gap tuning. Regarding interatomic distances between H-free carbon atoms, they on average are around 1.39 Å for dimerized C pairs, and 1.43 Å for undimerized pair, although these distances depend on the position of the C atom with respect to those carbon atoms, which are bonded to hydrogen.

4 Charge density, band gap and optics To discuss the physics of the gap opening for partially hydrogenated graphene, we start with the charge density of graphene (no H) and show in Fig. 2 (upper panel) charge density distribution for the DBs p_z orbitals. It is calculated 0.7 Å above the top C atoms, which corresponds to carbon covalent radius. Darker regions of the graph show higher electron charge density and it is practically zero in the center of

the C carbon rings. It can be seen from the figure that the electrons from DBs are delocalized along the C bonds around the rings, which is compatible with metallic behavior of the graphene and its zero band gap. On the other hand, remaining C atom orbitals within the plane of the graphene sheet are mostly of sp^2 type and form covalent bonding between the atoms (not shown).

Graphane is a direct gap material, for which both electron and optical gaps are the same. This is not a case for most of the partially hydrogenated systems we considered, they usually demonstrate indirect optical gap. As it was mentioned, however, experimentally produced partially hydrogenated systems should be disordered, therefore the gap, derived from the DOS or optical response, has to be considered when comparing with the experiment results. However, electron band gap obtained from the calculated electron structure can be very useful as an example to interpret, *e.g.*, optical response origin in terms of transition matrix elements and wave function symmetry between initial and final optical states.

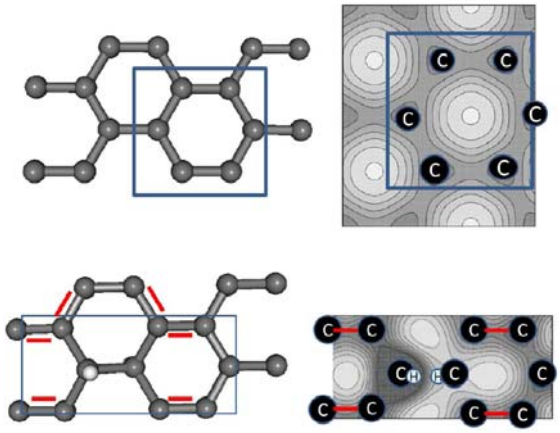

Figure 2 Top view on the atomic structure and charge density distribution of the p_z atomic orbitals 0.7 Å above the atomic plane for graphene (top) and $C_{16}H_2$ system (bottom). Square or rectangular (at the left), projected to the atomic structures, correspond to the area, at which the charge density is calculated and shown at the right. Mostly homogeneous distribution of the charge density indicates the delocalization of the electrons.

We do not discuss here the optical response of graphene, which is well documented, for details we address the reader to [28], where alongside with DFT LDA, both many-particle GW and excitonic effects were included. We will rather focus on a comparison of DFT LDA dielectric function of graphane and $C_{16}H_2$ structure.

The imaginary part of the dielectric functions ε_2 for graphane and $C_{16}H_2$ structures are shown in Fig. 3, top and lower panels respectively. The *xx* component (identical to *yy* component for graphane) and *zz* component are presented in the upper panel. For $C_{16}H_2$, its components *xx*, *yy* and *zz* are shown at the bottom. The imaginary part of the dielectric function system demonstrates fundamental difference in the optical transition for two systems. The wave functions symmetry of graphane is such that the noticeable optical transitions start well above the direct optical gap in high UV spectral energy range, and the optical response is isotropic along the carbon plane. In [11] the optical theory has been extended to include the GW and excitonic corrections, and the conclusions related to the optical transitions directly above the gap are identical to that one of DFT LDA, that we are using: there is a large delay in the energy, compared to the direct optical gap, when noticeable absorption starts. Such delay is around 4 eV for the light polarized along the graphane plane and about 3 eV for the light, polarized along *z* direction. Such energy already corresponds to ultraviolet range and makes the standard optical techniques not very useful for such a material. In a stark contrast, partial H coverage drastically modifies such symmetry, leading to substantial and *anisotropic* light absorption immediately *above the gap*.

As it is follow from the projected DOS (PDOS) [29], such a delay in the optical adsorption for graphane is mostly due to dominant *p* symmetry of the wave functions close to both the bottom of the valence band and the top of the conductivity band. This leads to very small or even vanishing transition matrix elements in the vicinity of the optical gap. One of the strong modifications of the optical adsorption induced by a partial H coverage is that the optical adsorption starts right away after the photon energy is above the band gap because wavefunctions of the initial and final state contain now both *p* and *s* components.

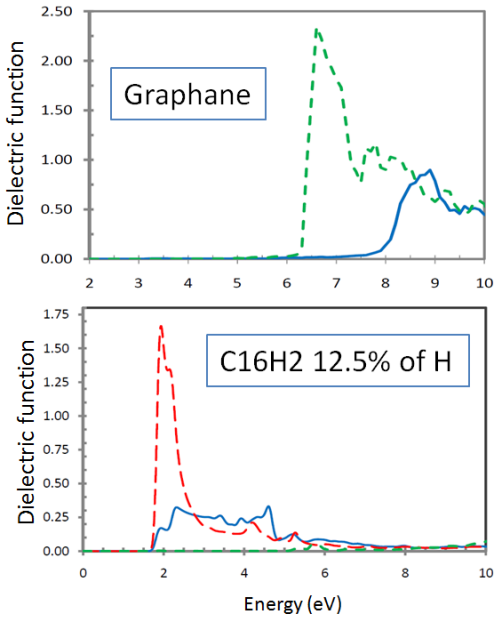

Figure 3 Dielectric function components (solid line: ε_{xx}, long dashes: ε_{yy} and short dashes: ε_{zz}) for graphane (top panel) and $C_{16}H_2$ structure (at the bottom). For $C_{16}H_2$ system DOS gap is 0.8 eV, while optics shows that the transitions start right after phonon energy reaches the direct energy gap (~1.43 eV).

Finally, the above graphs demonstrate that optical techniques will not only make easy detection of hydrogenation, but can also be used to decode the optical signal in terms of the structure, H ordering, gap modification, *etc*.

5 Conclusions It was proven theoretically that a variable electron band gap between that of graphene (0 eV) and its 100% hydrogenated counterpart graphane (5 eV) can be achieved through the partial hydrogenation of graphene, The results are in agreement with other theoretical investigation of the similar system. However, we focus here on fine details of the hydrogen induced atomic structure, electron transfer and their modification of the optical transitions for a few promising structural arrangements. This allowed us to demonstrate that the optical tools can be used to get microscopic access to the fine details of the hydrogenation processes. Out of the various structures considered, the example $C_{16}H_2$ "row close" arrangement (and systems, similar to that) was the one that would be appropriate for 2D microelectronics based on its band gap. In addition, other structures with a gap within 0.2–2.0 eV were produced and investigated.

We determined the main physical mechanisms of partial hydrogenation of graphene, which opens the gap: low hydrogen coverage causes both *buckling* and *dimerization* of carbon host atoms, leading to electron localization and thus the opening of the gap. The next steps for this research are modelling the electronic properties of partially hydrogenated graphene bi-layers and partially hydrogenated graphene on a substrate, including the linear and nonlinear optical response for *in-situ* characterization of the hydrogenation process, which is directed towards possible application in 2D microelectronics.

Acknowledgements The authors acknowledge the support from the Natural Sciences and Engineering Research Council of Canada (NSERC) and the Shared Hierarchical Academic Research Computing Network (SHARCNET). A.I.S. acknowledges Centro de Investigaciones en Optica, Leon, Mexico for the support during a partial sabbatical visit.

References

[1] K. S. Novoselov, A. K. Geim, S. V. Morozov, D. Jiang, Y. Zhang, S. V. Dubonos, I. V. Grigorieva, and A. A. Firsov, Science **306**, 666 (2004).
[2] C. Riedl, C. Coletti, T. Iwasaki, A. A. Zakharov, and U. Starke, Phys. Rev. Lett. **103**, 246804 (2009).
[3] D. A. Siegel, C. G. Hwang, A. V. Fedorov, and A. Lanzara, Phys. Rev. B **81**, 241417 (2010).
[4] A. Mattausch and O. Pankratov, Phys. Rev. Lett. **99**, 076802 (2007).
[5] P. Shemella and S. K. Nayak, Appl. Phys. Lett. **94**, 032101 (2009).
[6] P. R. Wallace, Phys. Rev. **71**, 622 (1947).
[7] D. C. Elias, R. R. Nair, T. M. G. Mohiuddin et al., Science **323**, 610 (2009).
[8] J. Katoch, J. Chen, R. Tsuchikawa, C. W. Smith, E. R. Mucciolo, and M. Ishigami, Phys. Rev. B **82**, 081417 (2010).
[9] B. Sachs, T. O. Wehling, A. I. Lichtenstein, and M. I. Katsnelson, Chap. Theory of Doping: Monovalent Adsorbates, p. 31, in: Physics and Applications of Graphene - Theory, edited by S. Mikhailov (InTech, 2011); URL: http://www.intechweb.org/books/show/title/physics-and-applications-of-graphene-theory.
[10] J. O. Sofo, A. S. Chaudhari, and G. D. Barber, Phys. Rev. B **75**, 153401 (2007).
[11] P. Cudazzo, C. Attaccalite, I. V. Tokatly, and A. Rubio, Phys. Rev. Lett. **104**, 226804 (2010).
[12] C. Berger, Z. Song, X. Li et al., Science **312**, 1191 (2006).
[13] M. Y. Han, B. Ozyilmaz, Y. Zhang, and P. Kim, Phys. Rev. Lett. **98**, 206805 (2007).
[14] P. G. Silvestrov and K. B. Efetov, Phys. Rev. Lett. **98**, 016802 (2007).
[15] H. Xiang, E. Kan, S. Wei, M. Whangbo, and J. Yang, Nano Lett. **9**, 4025 (2009).
[16] J. Cai, P. Ruffieux, R. Jaafar et al., Nature **466**, 470 (2010).
[17] D. W. Boukhvalov, M. I. Katsnelson, and A. I. Lichtenstein, Phys. Rev. B **77**, 035427 (2008).
[18] L. Zhu, H. Hu, Q. Chen, S. Wang, J. Wang, and F. Ding, Nanotechnology **22**, 185202 (2011).
[19] D. Haberer, C. E. Giusca, Y. Wang et al., Adv. Mater. **23**, 4497 (2011).
[20] P. Chandrachud, B. S. Pujari, S. Haldar, B. Sanyal, and D. G. Kanhere, J. Phys.: Condens. Matter **22**, 465502 (2010).
[21] A. I. Shkrebtii, J. L. Cabellos, N. Arzate, B. S. Mendoza, and P. McNelles, Controlled hydrogenation of graphene, graphene-like silicon and germanium by optical injection current, linear and nonlinear optics, International School of Solid State Physics, Epioptics-11, Erice, Sicily, 19-25 July 2010.
[22] D. Haberer, D. V. Vyalikh, S. Taioli et al., Nano Lett. **10**, 3360 (2010).
[23] R. Balog, B. Jorgensen, L. Nilsson et al., Nature Mater. **9**, 315 (2010).
[24] F. Gaspari, A. I. Shkrebtii, P. McNelles, J. L. Cabellos, and B. S. Mendoza, MRS Online Proceedings Library **1362**, mrss11-1362-qq09-18 (2011).
[25] P. Weightman, D. S. Martin, R. J. Cole, and T. Farrell, Rep. Progr. Phys. **68**, 1251 (2005).
[26] Quantum Espresso, http://www.quantum-espresso.org, 2007.
[27] F. Bechstedt, Principles of Surface Physics (Springer-Verlag, Berlin, 2003).
[28] L. Yang, J. Deslippe, C. Park, M. L. Cohen, and S. G. Louie, Phys. Rev. Lett. **103**, 186802 (2009).
[29] A. I. Shkrebtii (private communication).